Investigation of AlBN Grown by MOVPE

Oliver Rettig

In this report, growth of boron containing layers and their characterisation will be presented. Different growth parameters are changed to investigate whether they have beneficial influence on the growth of boron containing Al(Ga)N with boron contents in the percentage regime. As template previously optimised AlN layers with a thickness of 500 nm were mainly used for overgrowth.

1. Introduction

LEDs based on GaN material already revolutionised the light market in the visible spectrum. However, current ultraviolet (UV) applications such as sterilization and disinfection of water and air [1, 2], phototherapy [1], flourescence analytical systems [2], bio-agent detection [3], spectrometry and currency validation [4] still use mercury containing lamps. Even though UV-LEDs have many advantages like their size and non-toxicity, they still suffer from external quantum efficiencies below 10 %.

Apart from carrier injection efficiency and light outcoupling, there are further important challenges in the realization of high efficiency devices. State-of-the-art AlN templates still exhibit many threading dislocations which decrease the efficiency drastically when penetrating the optically active quantum wells (QWs). They are generated as a consequence of the lattice mismatch of sapphire or silicon carbide (SiC), which are possible substrate materials, and the AlN template grown on top. Also the lattice mismatch of the AlN template and the AlGaN QWs leads to a significant decrease in luminescence. AlGaN QWs with a thickness of only a few nanometers grow strained on top of the AlN template. Due to the strong piezoelectrricity of AlGaN-based materials, an electric field is induced in the compressively strained QWs leading to a band tilt. This results in a decrease of the overlap integral of the electrons and holes which causes a decrease in radiative recombination as well as a decrease of the effective transition energy.

By introducing boron, which is the lightest and smallest group-III element, to state-of-the-art AlGaN-based material systems, another degree of freedom in lattice matching can be utilised. Therefore both, template quality as well as a reduction of the quantum-confined Stark effect (QCSE) in the QWs might be achieved by the incorporation of boron. According to current scientific knowledge only 5 % of boron would be enough to lattice match AlBN on SiC.

In this work, we try to clarify whether it is possible to grow $Al_xB_yGa_{1-x-y}N$ layers with good crystalline quality. Until now only few studies have been focussing on the growth of boron containing group-III-nitrides [5–7]. Important material properties such as the

composition dependence of the bandgap, lattice parameter for wurtzite-BN and ionisation energies of donors and acceptors are not yet known for this material. Due to its very low surface diffusion, parasitic gas phase reactions and poor solubility in AlGaN [5], growing high quality boron containing material has not yet been achieved. By introducing high temperatures of up to 1400 °C, optimising V/III-ratio, applying indium as surfactant and precursor alternation we try to increase the surface mobility of boron. For characterisation, photoluminescence spectroscopy (PL), X-ray diffraction (XRD), scanning electron microscopy (SEM), atomic force microscopy (AFM), secondary ion mass spectroscopy (SIMS), and transmission electron microscopy (TEM) are performed to steadily increase the quality of the layers.

2. Experimental Details

The MOVPE reactor used for this study is a low-pressure horizontal reactor (Aixtron AIX-200/4 RF-S) with a high-temperature susceptor kit enabling growth temperatures up to 1400 °C. All group-III-nitrides are grown on standard (0001) sapphire substrates with an offcut of 0.3° towards the m-plane. Trimethyl-aluminium (TMAl), trimethyl-gallium (TMGa), trimethyl-indium (TMIn), triethyl-boron (TEB) and ammonia are used as precursors.

For characterisation, a high resolution X-ray diffractometer (Bruker Discover D8) is used to check the crystal quality of the samples. Additionally aberration-corrected high-resolution TEM (AC-HRTEM) was performed by our project partners of the Central Facility of Electron Microscopy at Ulm University.

Photoluminescence spectroscopy is performed by using an argon fluoride excimer laser as excitation source which works at a wavelength of 193 nm. This part was supervised by the Institute of Quantum Matter, Semiconductor Physics Group at Ulm University.

3. Growth of Boron Containing AlN Layers

3.1 Growth at AlN growth conditions

Literature reports different values for the incorporation efficiency of boron in AlN [8, 9]. Therefore, first experiments were performed at standard AlN growth conditions [10] using different amounts of boron. In SEM, we found that a boron content in the gas phase larger than 2 % drastically decreases the surface morphology. For TEB/III-ratios between 3 % and 29 %, no boron related XRD signal and a clearly visible shift of the PL defect band can be observed. In AlBN layers with higher boron content an additional defect band occurs at 4 eV which shifts even further to higher energies when increasing the boron supply. This band then dominates over the 3 eV defect band which is related to the AlN [11]. This already implies a change of growth regarding the formation of different defect types caused by boron.

In order to improve the layer quality, AlBN layers were grown with lower gas phase ratios of ~2 %. XRD as well as SIMS studies were performed to determine the amount of

boron incorporated in the AlBN layers. In XRD, a weak peak was visible in some layers which would indicate a boron content of only ~0.4 % can be calculated assuming fully relaxed layers and a c-lattice constant of 0.422 nm for w-BN [12]. Being very close to the AlN main peak at these low contents, the AlBN reflex only shows a weak response. In contrast, SIMS investigations identify 5 % of boron inside the layers which is much more than indicated by XRD measurements. Therefore further characterisations of the grown layers are performed. TEM investigations reveal columnar growth of the upper part of the AlBN. Figure 1 shows a weak beam dark field (WBDF)-TEM image in $g = 11\bar{2}0$ direction of the 300 nm thick AlBN layer grown on top of an AlN template with a thickness of 500 nm.

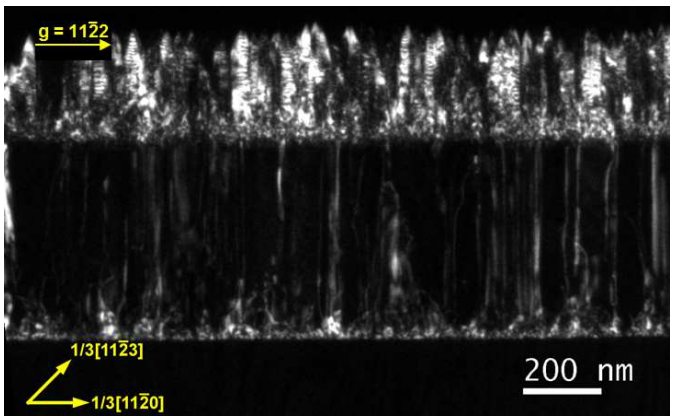

Fig. 1: WBDF image of a 300 nm thick $Al_{0.95}B_{0.05}N$ layer on top of a 500 nm thick AlN template on sapphire. For the upper part of the AlBN layer strong columnar growth can be observed.

The first ~50 nm of the AlBN show many bright small spots, which makes it impossible to follow the threading dislocations originating from the AlN template. In the upper part of the layer, strong columnar growth can be seen with many of those columns being bright whereas others appearing dark. The width of these columns fluctuates between 20 nm and 40 nm. As WBDF images are taken with a slight angle offset from the Bragg condition, only dislocations are visible as bright lines. Since in this image many of the columns are bright it can be concluded that they are rotated around the c-axis such that the crystal does fulfil the Bragg condition. Additionally a very rough surface can be observed for the AlBN layers. The individual columns have a very sharp tip resulting in a needle-like shape.

Selective area diffraction measurements (Fig. 2) of the interface of the AlN template show a wurtzite configuration of the AlBN, which matches the template well. Performing the same measurements at the top part of the AlBN, it can be seen that the wurtzite diffraction pattern smears up by a small amount. Course approximations of the angle suggest a tilt of the c-direction of ~4°.

Plan view TEM investigations of the top of the AlBN layer (Fig. 3) confirm strong columnar growth. In fact the columns do not coalesce completely to form a closed layer. In between those columns formation of amorphous material appears. Nevertheless, the diffraction pattern of the columns depicts crystallinity in wurtzite configuration. However a tilt

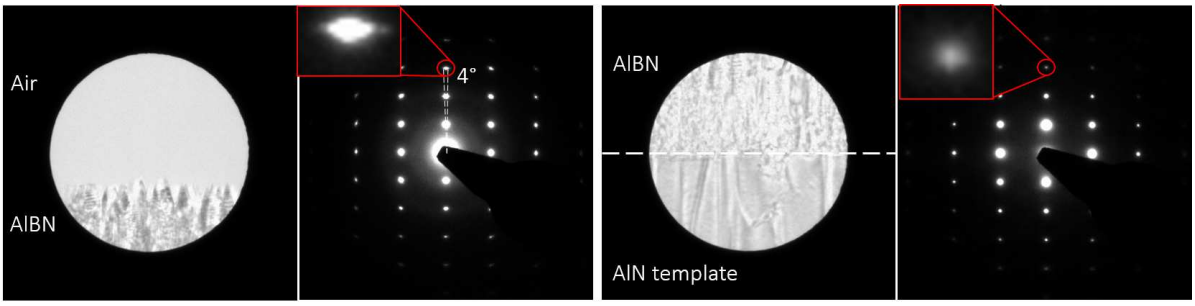

Fig. 2: Selective area electron diffraction image of the upper part of the AlBN layer with columnar growth and the interface between the AlN template and the AlBN layer. The c-axis of the AlBN columns at the top rotated up to 4°, whereas at the interface the lattice fits the direction of the template well.

of the columns by up to 3° around the c-axis can be observed. High resolution images of the coalescence region of two neighbouring columns after filtering respective lattice directions confirm the difference in lattice direction of ~2°.

The presence of strong columnar growth with amorphous material enclosed might be the reason for the inconsistency in SIMS and XRD data. Accumulation of boron in the amorphous materials due to phase separation causes less boron incorporation in the AlBN columns. Therefore XRD, which reflects the composition of the columns, can only measure much lower boron concentrations than SIMS, which is sensitive for the overall presence of boron, but cannot distinguish between material incorporated in the columns and material present in the amorphous inclusions.

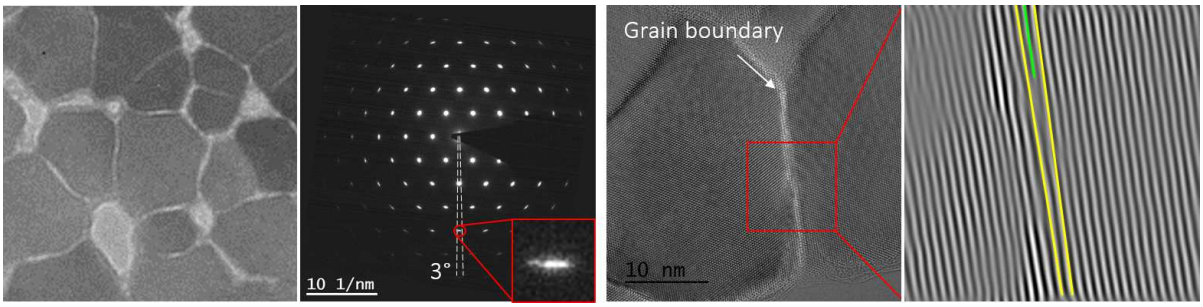

Fig. 3: Plan view TEM images and electron diffraction pattern of surface near region of the AlBN layer. A non-fully-coalesced layer of individual columns can be observed. Diffraction patterns reveal a rotation of the crystal structure around the c-axis of the columns by up to 3°. This behaviour can be validated by high resolution images of neighbouring columns where a tilt of ~2° is visible.

3.2 High-temperature growth series

From literature [5] and the results obtained above we conclude that the surface mobility of the boron is the main reason for columnar growth since the columns do not coalesce to

form a closed layer. Hence, further studies were performed trying to increase the mobility of the B atoms on the growing surface.

By using a high-temperature setup for our MOVPE reactor, it is possible to reach temperatures up to 1400 °C. To investigate whether high temperatures help to improve crystal growth, a series with 3 different temperatures was grown, not changing any other process parameters. Figure 4 shows PL spectra of 300 nm thick AlBN layers grown on the same 500 nm thick AlN template which is also displayed as reference.

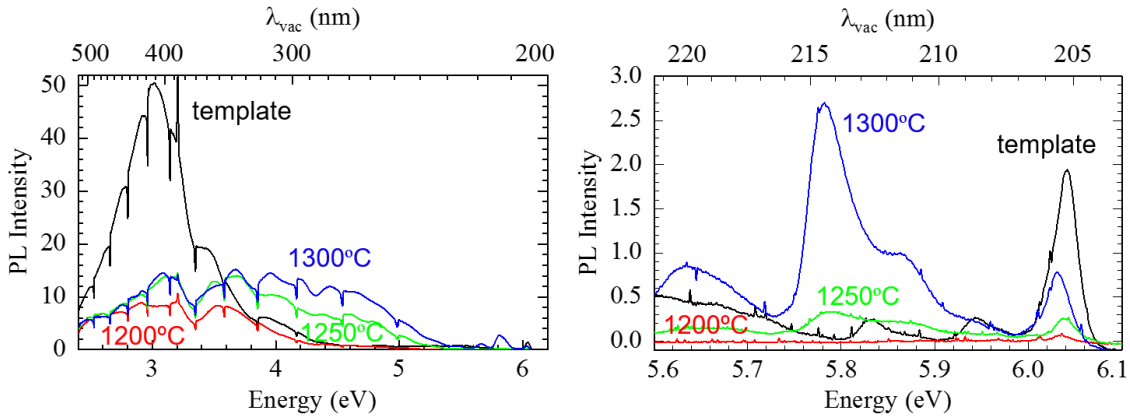

Fig. 4: Overview PL spectra of AlBN temperature series and reference template (left) and zoomed NBE region (right). With higher temperatures an additional defect band arises at around 4 eV. At high temperatures the NBE luminescence also exhibits additional contributions.

One can clearly see a drop in intensity in the defect related PL intensity when boron is supplied during growth. Moreover, a change in the respective positions of the peaks can be observed. All 3 AlBN layers still show a contribution at 3 eV which is most likely related to the AlN defect band. Additionally, a second contribution is present for all boron containing samples. Those peaks however are not appearing at the same energy for all samples. With increasing temperature the centre of the peak shifts to higher energies. At 1200 °C this peak is located at ~3 eV whereas at 1300 °C a much broader peak is visible reaching from 3.6 eV up to 5 eV. Previous studies showed a similar behaviour of the defect band when increasing the boron supply in the gas phase, leading to the conclusion that at higher temperatures more boron incorporated in the AlBN layers might be present compared to lower temperatures. However SIMS measurements revealed that more boron is incorporated in layers grown at lower temperatures. Again it has to be considered that this does not necessarily mean an increase in boron incorporation in the crystalline parts of the layers.

In the near-band-edge (NBE) region the PL spectra of the AlBN layers differ significantly. Whereas the layer grown at 1200 °C shows almost no NBE luminescence, different major contributions are visible in the spectra of the samples grown at 1300 °C surface temperature. The latter shows much stronger AlN-related band-edge luminescence. Additionally, a very strong peak arises at 5.8 eV. For this peak, different origins are possible. When considering bandgap bowings reported in literature [13] a boron content below 5 % can

lead to a decrease in the bandgap energy by up to 300 meV which is in good agreement with the data received by SIMS investigations. However bowing parameters as well as band-edge energies of wurtzite BN are still not well known and contradictory discussed in literature due to its unstable nature. Another possible origin of this contribution is the presence of hexagonal BN. Due to phase separation at higher temperatures BN might grow in its initially more stable hexagonal phase. As discussed in [14], an indirect bandgap of h-BN with the longitudinal and acoustic phonon transitions present at energies possibly related to $Al_{0.95}B_{0.05}N$. The strong PL peak at ~5.8 eV in Fig. 4 might be related to optical phonons. The acoustic phonons should have a contribution at ~5.86 eV, which fits well with our PL data. The respective ratios between acoustic and optical phonons should be constant for all samples. This, however, could not be verified for additional grown layers runs, indicating that this peak might be related to other phenomena. TEM diffraction patterns of the hotter grown layers, which are not displayed here, reveal that the wurtzite crystallinity of the previous layers (see Fig. 2) cannot be maintained. Therefore it has to be assumed that at higher temperatures, phase separation is preferred over the incorporation in AlN, leading to other possible phases like h-BN or amorphous growth.

3.3 Reduction of boron supply

With the goal to achieve growth of a closed layer without having strong columnar features present, a further decrease in boron content in the gas phase was performed. Boron contents reported here arise from the assumption of linear incorporation with gas phase supply, starting at boron contents known from our previous SIMS investigations. A growth temperature of 1170 °C was chosen in order to suppress the additional NBE contributions observed in Sect. 3.2.

It is clearly visible that changing the boron supply does not affect the shift of the NBE peak. Only the intensity of the peaks increases by the reduction of boron. The small down-shift in energy of the band edge might be related to the boron incorporated in the AlBN layers. Again utilising bowing parameter values reported in literature [13], this shift would be related to approximately 0.4 % of boron in AlN. However those values are still vague due to the scarce literature available for boron containing III-nitrides. Nevertheless, from the position of the band edge being constant for all boron contents, it could be concluded that the solubility limit of boron in AlN is reached for respective growth conditions. This assumption would also fit with previous investigations of strong columnar growth and amorphous material grown between the columns. Excessive boron which cannot be incorporated in AlN accumulates and forms amorphous clusters.

4. Summary

First studies on the growth of boron containing AlN layers were performed. $Al_{0.95}B_{0.05}N$ was grown with strong columnar growth as well as growth of amorphous material could be observed. The columns show wurtzite configuration in TEM investigations. From our studies we conclude that phase separation might be caused by exceeding the solubility of boron in AlN.

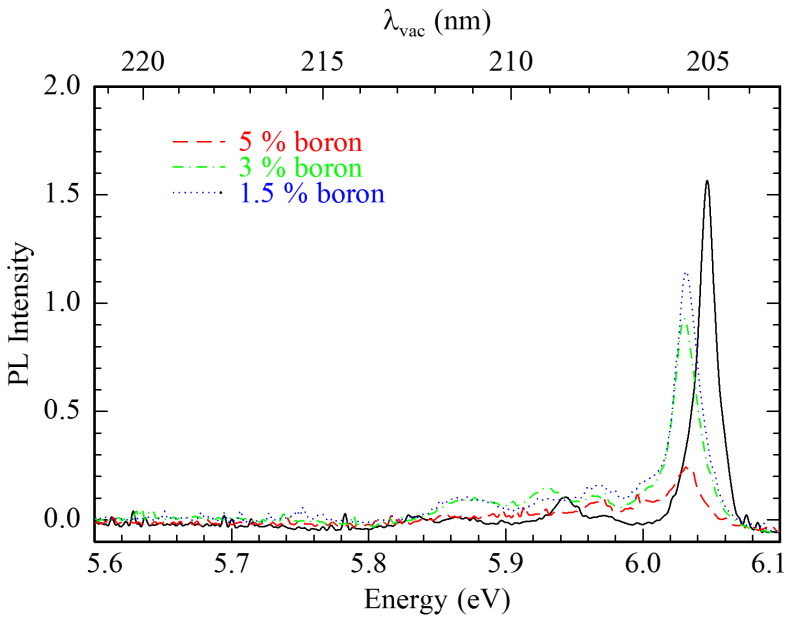

Fig. 5: NBE PL spectra of AlBN boron series and their template as reference. The amount of boron between 1.5 % and 5 % supplied during growth, does not affect the shift of the band edge related peak.

Therefore, more experiments are currently planned to decrease the boron content further to reach a concentration that is still below the solubility limit. Additionally, by optimising the growth conditions, we try to increase it further.

Acknowledgment

I thank the coauthors J.-P. Scholz, S. Bauer, M. Hocker, and K. Thonke of the Institute of Quantum Matter, Semiconductor Physics Group at Ulm University, Y. Li, H. Qi, J. Biskupek, and U. Kaiser of the Central Facility of Electron Microscopy at Ulm University, and T. Hubáček of the Institute of Physics, Czech Academy of Sciences, Prague, Czech Republic for their scientific support. This work was financially supported by the DFG within the framework of the project "Investigations on the epitaxy of AlBGaN heterostructures for applications in UV-LEDs".

References

[1] M. Kneissl, T. Kolbe, C. Chua, V. Kueller, N. Lobo, J. Stellmach, A. Knauer, H. Rodriguez, S. Einfeldt, Z. Yang, N.M. Johnson, and M. Weyers, "Advances in group III-nitride-based deep UV light-emitting diode technology", *Semicond. Sci. Technol.*, vol. 26, pp. 014036-1–6, 2011.

[2] H. Hirayama, S. Fujikawa, N. Noguchi, J. Norimatsu, T. Takano, K. Tsubaki, and N. Kamata, "222–282 nm AlGaN and InAlGaN-based deep-UV LEDs fabricated on high-quality AlN on sapphire", *Phys. Status Solidi A*, vol. 206, pp. 1176–1182, 2009.

[3] X. Hu, J. Deng, J.P. Zhang, A. Lunev, Y. Bilenko, T. Katona, M.S. Shur, R. Gaska, M. Shatalov, and A. Khan, "Deep ultraviolet light-emitting diodes", *Phys. Status Solidi A*, vol. 203, pp. 1815–1818, 2006.

[4] C. Pernot, M. Kim, S. Fukahori, T. Inazu, T. Fujita, Y. Nagasawa, A. Hirano, M. Ippommatsu, M. Iwaya, S. Kamiyama, I. Akasaki, and H. Amano, "Improved efficiency of 255–280 nm AlGaN-based light-emitting diodes", *Appl. Phys. Express*, vol. 3, pp. 061004-1–3, 2010.

[5] T. Akasaka and T. Makimoto, "Flow-rate modulation epitaxy of wurtzite AlBN", *Appl. Phys. Lett.*, vol. 88, pp. 041902-1–3, 2006.

[6] A.Y. Polyakov, M. Shin, W. Qian, M. Skowronski, D.W. Greve, and R.G. Wilson, "Growth of AlBN solid solutions by organometallic vapor-phase epitaxy", *J. Appl. Phys.*, vol. 81, pp. 1715–1719, 1997.

[7] M. Kurimoto, T. Takano, J. Yamamoto, Y. Ishihara, M. Horie, M. Tsubamoto, and H. Kawanishi, "Growth of BGaN/AlGaN multi-quantum-well structure by metalorganic vapor phase epitaxy", *J. Cryst. Growth*, vol. 221, pp. 378–381, 2000.

[8] X. Li, S. Sundaram, Y.E. Gmili, T. Moudakir, F. Genty, S. Bouchoule, G. Patriarche, R.D. Dupuis, P.L. Voss, J.P. Salvestrini, and A. Ougazzaden, "BAlN thin layers for deep UV applications: BAlN thin layers for deep UV applications", *Phys. Status Solidi A*, vol. 212, pp. 745–750, 2015.

[9] T. Takano, M. Kurimoto, J. Yamamoto, and H. Kawanishi, "Epitaxial growth of high quality BAlGaN quaternary lattice matched to AlN on 6H-SiC substrate by LP-MOVPE for deep-UV emission", *J. Cryst. Growth*, vol. 237, pp. 972–977, 2002.

[10] O. Rettig, "Investigation of AlBGaN structures for UV-lighting", *Annual Report 2016*, pp. 65–70, Ulm University, Institute of Optoelectronics.

[11] K. Genji and T. Uchino, "Time-resolved photoluminescence characterization of oxygen-related defect centers in AlN", *Appl. Phys. Lett.*, vol. 109, pp. 021113-1–5, 2016.

[12] A. Nagakubo, H. Ogi, H. Sumiya, K. Kusakabe, and M. Hirao, "Elastic constants of cubic and wurtzite boron nitrides", *Appl. Phys. Lett.*, vol. 102, pp. 241909-1–5, 2013.

[13] S. Azzi, A. Zaoui, and M. Ferhat, "On the importance of the band gap bowing in boron-based III-V ternary alloys", *Solid State Comms.*, vol. 144, pp. 245–248, 2007.

[14] G. Cassabois, P. Valvin, and B. Gil, "Hexagonal boron nitride is an indirect bandgap semiconductor", *Nature Photonics*, vol. 10, pp. 262–266, 2016.